

Two-phase strategy of neural control for planar reaching movements: I. XY coordination variability and its relation to end-point variability

Miya K. Rand · Yury P. Shimansky

Received: 17 July 2012 / Accepted: 13 November 2012 / Published online: 30 November 2012
© Springer-Verlag Berlin Heidelberg 2012

Abstract A quantitative model of optimal transport–aperture coordination (TAC) during reach-to-grasp movements has been developed in our previous studies. The utilization of that model for data analysis allowed, for the first time, to examine the phase dependence of the precision demand specified by the CNS for neurocomputational information processing during an ongoing movement. It was shown that the CNS utilizes a two-phase strategy for movement control. That strategy consists of reducing the precision demand for neural computations during the initial phase, which decreases the cost of information processing at the expense of lower extent of control optimality. To successfully grasp the target object, the CNS increases precision demand during the final phase, resulting in higher extent of control optimality. In the present study, we generalized the model of optimal TAC to a model of optimal coordination between *X* and *Y* components of point-to-point planar movements (XYC). We investigated whether the CNS uses the two-phase control strategy for controlling those movements, and how the strategy parameters depend on the prescribed movement speed, movement amplitude and the size of the target area. The results indeed revealed a substantial similarity between the CNS’s regulation of TAC and XYC. First, the variability of XYC within individual trials was minimal, meaning that execution noise during the movement was insignificant. Second, the inter-trial variability of XYC was considerable during the

majority of the movement time, meaning that the precision demand for information processing was lowered, which is characteristic for the initial phase. That variability significantly decreased, indicating higher extent of control optimality, during the shorter final movement phase. The final phase was the longest (shortest) under the most (least) challenging combination of speed and accuracy requirements, fully consistent with the concept of the two-phase control strategy. This paper further discussed the relationship between motor variability and XYC variability.

Keywords Optimal control · Motor variability · Coordination variability · Kinematics

Introduction

Movement optimization and two-phase coordination strategy

In the last decade, applications of an optimality approach to limb movement trajectory have been useful for the general understanding of the neural control of reaching-type movements. Despite the fact that movement control optimality is a rather powerful theoretical concept, it has not been developed yet into a comparably useful instrument for quantitative analysis of experimental data. In an attempt to do so, we recently utilized an optimality approach to describing transport–aperture coordination (TAC) during reach-to-grasp movements (Rand et al. 2008, 2010b). Specifically, we developed a model of an optimal relationship between experimentally observed variables of movement dynamics without explicitly solving an optimal control problem.

The main ideas behind our novel approach are outlined in the following. If the control system is optimal, there is

M. K. Rand (✉)
IfAdo-Leibniz Research Centre for Working Environment
and Human Factors, Ardeystraße 67, 44139 Dortmund, Germany
e-mail: rand@ifado.de

Y. P. Shimansky
School of Biological and Health Systems Engineering,
Arizona State University, Tempe, AZ 85287-9709, USA

tight coordination between independently controlled processes that are required to finish simultaneously with each other. Hand transport and grasping components of a reach-to-grasp movement are two such processes. Since reach-to-grasp is well-trained through daily activities, an optimality approach is fully applicable to it (Hoff and Arbib 1993). Therefore, the control dynamics must obey Bellman–Pontryagin equations (Naslin 1969). From those equations, a smaller set of equations describing optimal coordination between hand transport and grasp aperture can be obtained (see derivation in Appendix section “[Derivation of experimentally verifiable equations describing optimal coordination](#)”). Those equations hold for every moment in movement time provided that movement control is fully optimized. They constitute a representation (i.e., a model) of an optimal relationship between movement variables that are directly measured or computed from experimental data. A universal approximator (e.g., an artificial neural network) can be used to best fit the model to the experimental data (i.e., all time frames from all trials which are assumed to have been performed in an optimal way under a specific condition). Once the unknown coefficients of that model are identified through the best fitting, the model of optimal coordination is completely defined. A very important advantage of our novel approach is that it does not require knowing detailed information about the controlled object’s dynamics or the optimality criterion for establishing an optimal coordination model.

Another important advantage is that the model can be used as a tool for quantifying the extent of the deviation of the experimentally observed relationship among movement variables from optimality: The smaller the residual errors of model fitting, the higher the fitting precision and the closer the motor coordination to an optimal pattern. At the same time, from the perspective of motor variability, that deviation is a manifestation of the variability of coordination-specific relationship among movement variables included in the optimal model, and hence, it can be termed *coordination variability*. It should be emphasized that, since the control of multicomponent coordination is rather complex and some variability types significantly affect task performance while some others do not (Darling and Stephenson 1993; Valero-Cuevas et al. 2009), an accurate assessment of coordination optimality requires a quantitative model of optimal coordination. Consequently, such coordination variability cannot be observed as traditionally studied trajectory variability. The extent of coordination variability can be quantified not only for a specific movement phase across different trials, but also within one trial. Coordination variability computed across different trials is termed *inter-trial* coordination variability and that computed within a trial is termed *intra-trial* coordination variability.

We have applied the above optimal coordination model approach to studying reach-to-grasp movement. The utilization of that approach has been proven very useful for analyzing the experimental data obtained in human individuals (healthy persons and individuals with Parkinson’s disease) under various conditions (e.g., Rand et al. 2006, 2008, 2010a, b, 2012). We found that an inter-trial variability of TAC was significant during the aperture-opening phase (from movement onset to maximum grip aperture), but minimal during the aperture closure phase (from maximum grip aperture to contact with the target object). Based on those findings, we came to a conclusion that the CNS utilizes a two-phase strategy of controlling TAC during reach-to-grasp movements (Rand et al. 2010b). According to the two-phase control strategy, the cost of information processing during motor planning and movement online control is saved during the initial phase of movement at the account of reduced precision (and, therefore, reduced cost) of neural computations. In the final phase of movement control, that precision is significantly increased to ensure sufficient precision at the end-point of the movement trajectory. We also found that an intra-trial variability of TAC was very small, indicating that the precision of TAC is rather high. It also means that execution noise is insignificant.

Generalization of TAC model of reach-to-grasp movements to XY coordination (XYC) of reaching movements

We have hypothesized that such two-phase strategy is also used for controlling other reaching-type movements (Shimansky and Rand 2012) as long as the following conditions are satisfied. First, reasonably high precision of a contact with the target object at the end of transport is required. Second, the transport component of task performance is sufficiently long, so that saving the cost of neural computations during the initial phase of movement control is worthwhile. Third, the participants are well-trained on performing the task, meaning that the performance is sufficiently optimized and well coordinated.

The present study tests this hypothesis in experiments on reaching performed in a 2-D space (X – Y horizontal plane) by examining coordination between X and Y movement components. Each component is described by three movement parameters: position, velocity and acceleration (six parameters in total). For this purpose, a model describing an optimal relationship between the six movement parameters is fitted to experimental data for estimating the variability of XY coordination (XYC) and determining how close XYC is to optimality. The X and Y hand motion components are controlled by highly overlapping muscle sets. However, from the perspective of

mechanics, they correspond to mutually independent degrees of freedom. In accurate reach-to-point 2-D movements, there is a requirement that the movement components corresponding to X and Y coordinates finish simultaneously. Thus, one can expect to observe tight coordination between controlling those components.

The current study is focused on investigating whether inter-trial variability of XYC during planar reaching movements has features characteristic for the two-phase control strategy, and also whether those features are similar to the analogous features of TAC observed during reach-to-grasp movements. This study further examines how the end-point variability of movement trajectory influences the inter-trial variability of XYC .

Methods

Participants

Fifteen young adults participated in this study (mean age \pm SD: 25.9 ± 2.6 ; 7 males and 8 females). They were all right-handed and with no known neuromuscular deficits. All participants provided written informed consent prior to participation.

Apparatus and procedure

Participants sat comfortably in a chair in front of a table on which a digitizer tablet (Wacom Intuos 4 XL) was placed. Participants held a stylus in a manner similar to holding a pen for hand writing and made single-stroke arm movements, during which both the stylus's tip and the hand were continuously contacting with the digitizer's surface. The digitizer tablet sampled the X position and Y position of the tip of the stylus with a frequency of 133 Hz and a spatial resolution of 0.005 mm. The digitizer was linked to a computer, which generated an auditory signal to move and stored the data. A program written in Matlab was used for data acquisition.

All participants performed twelve types of single-stroke arm movements in the horizontal plane from the starting area (a circle 1 cm in diameter) to the target area (also a circle). The size of the starting area was the same throughout the experiment. The starting position and the target were aligned along the participants' midline and displayed throughout a trial. The movement amplitude, target size and movement speed were varied across twelve conditions. There were two different reaching distances: 15 cm (short-distance condition) and 30 cm (long-distance condition). Two different target sizes were used: a circular area of 2.1 cm in diameter (large-target condition) and 0.7 cm in diameter (small-target condition). There were three movement speed conditions [low (i.e., low),

comfortable (i.e., normal), and as high as possible (i.e., maximum)]. Two target distances and two target sizes were combined with the three movement speeds to produce twelve possible conditions, which were randomized based on a random number generator.

Participants were instructed to move the stylus (i.e., sliding the tip of the stylus on the digitizer's surface) from the starting position to the target location at a required speed. At the start of each trial, the participants positioned the tip of the stylus in the starting position, and the examiner said "ready." After a random delay (between 1 and 2 s), an auditory go-signal was delivered. In response to the go-signal, the participants initiated the movement. For each condition, participants made a few practice trials and subsequently performed a block of twelve trials under each condition; data analysis was based on the last ten trials.

The movement path was recorded and displayed on the computer monitor, which allowed the examiner to determine whether the trial was executed properly. Trials were rejected if the participant either missed the target or exhibited obvious hesitation before entering the target area. When participants overshot the target, a loud beep sound was produced to notify them of this error. These rejected trials were redone at the end of each condition. The average number of rejected trials across participants was 0.7 (low-speed), 0.7 (normal-speed) and 0.4 (maximum-speed) trials for the (large-target, short-distance) combination of conditions, and 1.0 (low-speed), 1.2 (normal-speed), and 1.3 (maximum-speed) trials for the (large-target, long-distance) combination. The comparable numbers were 0.8, 0.8 and 2.9 trials for the small-target and short-distance conditions, and 1.7, 0.5 and 2.9 trials for the small-target, long-distance conditions. Data from 120 trials (10 trials \times 12 conditions) for each participant were analyzed.

Data analysis

Reaching-to-point movement was assessed based on the X and Y coordinates of the stylus tip on the digitizer (called *hand position* in the rest of the text). Hand velocity and acceleration were calculated as the first and second derivative of hand position, respectively. The derivatives were calculated based on the sliding window technique, where the data points within the window (the window width was 7 points) were approximated with a quadratic polynomial. The polynomial was then used for calculating analytic derivative at the window's center (or other points, when at the beginning or end of the data array representing the curve). Thus, calculating derivatives using this method also provided data filtering.

Movements were performed mostly along the X coordinate. Calculations of the onset and the offset of the reaching movements were performed by an automated

movement parsing algorithm (Teasdale et al. 1993, algorithm B). These points in time were first automatically detected using computer software. Subsequently, the results of this automatic procedure were inspected and corrected manually as needed. To obtain general characteristics of reaching movements, movement time was calculated for each trial. Average hand velocity was also computed for each trial across the entire movement period as a ratio between the vector distance travelled by the hand and the corresponding movement time. For each of these parameters, the mean value across the ten trials was calculated for each of the experimental conditions for each participant. Statistical comparison of these parameters between experimental conditions was performed by using a 2 (target size: large, small) \times 2 (reaching distance: short, long) \times 3 (movement speed: low, normal, maximum) ANOVA with repeated measures. When appropriate, post hoc analysis was carried out using the *t* test with Bonferroni adjustments.

To investigate the factors influencing the end-point variability as well as the relationship between inter-trial variability of XYC and general variability of reaching movements, the variability of hand position was measured both at the beginning and the end of the movement. For this purpose, the standard deviation of hand starting and final positions across trials was measured separately for the *X* and *Y* coordinates for each condition for each participant. In addition, the variability of movement direction was calculated at 3 cm from the initial position of the hand.¹ For this purpose, the initial movement direction was characterized by the angle between the *x* axis and the straight line segment connecting the starting hand position and the hand position along the movement trajectory immediately past 3 cm distance from the starting position. The standard deviation of that angle across trials was determined separately for each participant under each condition. All of these standard deviation values were

¹ Initial movement direction is often measured at a certain time after the movement onset, such as 100 ms (Bernier et al. 2005; Hinder et al. 2010) and 200 ms (Heuer and Hegele 2008), or at a certain kinematic landmark, such as peak velocity (Hinder et al. 2010; Wang and Sainburg 2005). The average distance of hand position at 180 ms into movements from the movement onset was 3.3 mm for the small-target, short-distance, slow-speed condition and 56.0 mm for the large-target, short-distance, maximum-speed condition. This wide range of the distance from the movement onset across different conditions prevented us from using a certain time from the movement onset or peak velocity for this measurement. It is because the initial direction measurement is unstable at a very short distance from the starting position (i.e., 3.3 mm) and because the angle of initial movement direction significantly varies depending on the distance from the starting position that is used for the measurement. Therefore, we employed a fix distance (3 cm), which was close to the average distance across the conditions at 180 ms into the movement.

subjected to the same 2 \times 2 \times 3 ANOVA described above for statistical comparisons.

Furthermore, to determine whether the end-point variability depended on the variability of the *X* and *Y* components of the initial position and the initial direction angle, a linear regression analysis was performed separately for the *X* and *Y* components of the end-point. For this analysis, each of these parameters was used as the dependent variable, and the *X* and *Y* components of the initial position and the initial direction angle were used as the independent variables. The correlation coefficients were statistically compared between experimental conditions according to the method described in (Papoulis 1990).

Utilization of the mathematical model of XY coordination

For analyses of XYC, the following six parameters were measured for each sampling point throughout the movement: (1) *X* position (*x*), (2) *X* velocity (v_x), (3) *X* acceleration (a_x), (4) *Y* position (*y*), (5) *Y* velocity (v_y) and (6) *Y* acceleration (a_y). Those six parameters were selected because they completely describe the two-dimensional dynamics of hand transport to the target.² Movements were performed mostly along the *X* coordinate.

To estimate XYC variability, all movements were normalized for each condition separately based on their respective average durations across all trials and all participants. The movement parameters (*x*, *y*, v_x , v_y , a_x , a_y) were then resampled with the original rate (133 Hz) so that the number of data points was the same in each trial for each participant under the same condition.

Optimal XYC in terms of the six parameters of hand transport was expressed in the form of the following linear equation (Model 1).

$$k_x x + k_y y + k_{v_x} v_x + k_{v_y} v_y + k_{a_x} a_x + k_{a_y} a_y = 0, \quad (1)$$

where k_x , k_y , k_{v_x} , k_{v_y} , k_{a_x} and k_{a_y} are constant weight coefficients, and *x*, *y*, v_x , v_y , a_x and a_y are centralized (by subtracting the mean) movement parameters. A formal mathematical derivation of a general form of this equation is provided in Appendix section “Derivation of experimentally verifiable equations describing optimal coordination”.

² To someone who is used to thinking about motor control in terms of kinematic parameters as continuous sequences of values within a specific time interval, it might seem that, since, for instance, acceleration as a function of time can be computed as a time derivative of velocity, it must be sufficient to include only one such parameter in equations. In the case of the equation describing XY coordination, however, *instantaneous* values of such parameters are involved, and therefore, a different logic applies. Knowledge of hand velocity at a certain time point *t* in general does not allow one to calculate hand acceleration and vice versa. For this reason, these kinematic variables are viewed in theoretical mechanics as state coordinates independent of each other.

The above simple linear approximation of optimal XYC has been selected because a linear approximation of the optimal transport–aperture coordination model was found to fit experimental data reasonably well (Rand et al. 2008, 2010b). The gist of the functional meaning of this model of an optimal relationship between the movement parameters can be explained as follows. It is well known that an optimal trajectory of point-to-point reaching movements is virtually a straight line (e.g., Viviani and Flash 1995; Shimansky et al. 2004). A general equation for a straight line (passing through the coordinates center) in 2-D is

$$k_x x + k_y y = 0, \quad (2)$$

which is a simplified version of Eq. 1. A more complex equation (i.e., Eq. 1) is needed to take into account the movement velocity and acceleration.

Evaluation of model fitting error

To estimate how close experimentally observed XYC was to optimality, Model 1 (Eq. 1) was fitted to different data subsets that corresponded to different movement phases. The procedure of model application to a specific data subset resulted in an estimate of the magnitude [root mean square (RMS)] of the residual errors of model fitting. In the case of XYC during reaching movement, there is no unique variable that can serve as a target (i.e., dependent variable) for linear regression. At the same time, for estimating the model's precision, it is necessary to determine how close a linear combination of those six parameters (with weights that are not all equal to zero) is to zero. Mathematically, this problem can be reduced to determining the least eigenvalue of the covariance matrix of those parameters: The closer it is to zero, the higher the precision of the linear model (e.g., Shimansky 2000). Then, the vector of (optimal) weight coefficients in Eq. 1 is simply the eigenvector corresponding to the least eigenvalue. That vector was used to obtain the model's fitting error for any specific vector of movement parameters (x, y, v_x, v_y, a_x, a_y).³ More detailed

³ It is important to acknowledge that the correlation matrix should not be, in general, used for this purpose. This is so because the variance of one or more movement parameters in general can be very small. For example, in the case of XY reaching movement, the stylus tip trajectory can be arranged along the x axis with negligible variation along the Y axis. In this example, the XYC model $k_y y - y_0 = 0$, where $k_y = 1$ and y_0 is the average Y coordinate, accurately describes the movement, since the variation of y around y_0 is very small. On the first sight, it may seem incorrect to state that an optimal XYC is observed in this example. However, simply by rotating the XY coordinate system 45 degrees (clockwise or counterclockwise), one can obtain a trajectory where any displacement along the x axis is almost exactly equal (in its absolute value) to the corresponding displacement along the Y axis, thus showing a near-perfect XYC. The method of determining the XYC model's precision obviously should not depend on the choice of the XY coordinate system.

explanations are provided in Appendix section “[Estimation of fitting errors for the XY optimal coordination model](#)”.

Based on the above considerations, the fitting error for the linear implementation of the XYC model was calculated as follows. First, the covariance matrix for the six movement parameters was calculated for the data subset to which the model was to be fit. Second, the eigenvalues of that matrix were determined (by using a standard procedure) and the fitting error was calculated as a square root of the smallest eigenvalue divided by the mean eigenvalue (across all the eigenvalues). The mean eigenvalue here represents the mean variance across the movement parameters.⁴ By taking the square root, the estimate of the fitting error magnitude was made compatible with the usual root mean square (RMS) measure of mismatch errors. Note that the obtained error estimate is dimensionless. Its upper bound is equal to 1, which corresponds to the absence of any correlation among the movement parameters. To make the error magnitude estimate insensitive to the differences between the variances of position, velocity and acceleration (e.g., due to the choice of units), the respective scaling coefficients were selected so that those variances (across the data set) were approximately the same. See more detailed explanations in Appendix section “[Estimation of fitting errors for the XY optimal coordination model](#)”.

Most of the data analysis in this study consists of applying Model 1 to different subsets of the entire data set within each condition, which includes the values of the above six movement parameters from all sampled time points and all trials within each participant. Whenever it is said below that Model 1 is applied to a specific data set, this means the above procedure unless explicitly stated otherwise. The usage of different data sets depending on analytical purposes is illustrated in Fig. 1. The RMS error of model fitting (i.e., residual error magnitude based on the least, sixth eigenvalue) was calculated for each data set.

Utilization of Monte-Carlo approach for achieving consistency of coordination variability measurement

In the next sections, the analysis of the variability of XYC within different movement phases is described. To determine the variability of XYC within a specific phase of the movement, the optimal coordination model (Model 1) was fitted to the data within a certain time window. The window width (i.e., duration) was specified as specific percentage of the total movement time (rather than specific time duration) to have the window correspond to a specific phase of the movement invariant with respect to

⁴ To see that, note that the total variance is equal to the sum of the diagonal elements (i.e., trace) of the covariance matrix, and the sum of the eigenvalues is equal to the above sum.

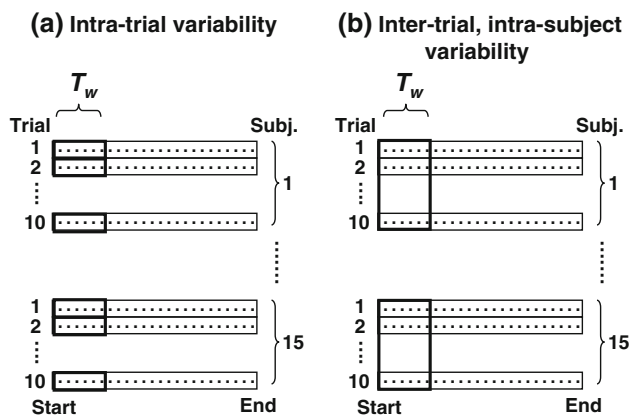


Fig. 1 Schematic diagrams of data sets used for model fitting to examine XY coordination (XYC) variability. For each condition, the XYC model was applied to a data set comprising data points within each trial separately (**a**) and across trials within each participant separately (**b**). Data sets are depicted by *thick-lined boxes*. For data sets plotted in **a**, a time window width (T_w) was set as equal to the average movement time. For data sets plotted in **b**, T_w was set as 20 % of the average movement time, and a sliding window technique for model fitting was used to examine the phase dependence of XYC variability. The time window was moved forward one data point at a time, and model fitting was performed at each step (on the data set within the window). See text for more details

movement time duration that varied considerably across different conditions. Thus, the number of data frames in such time windows also considerably varied between different experimental conditions. Even though all movements were initially normalized for each condition separately as described earlier (section “[Utilization of the mathematical model of XY coordination](#)”), the number of data frames in such time windows still varied across conditions. However, it is important to have the same number of data points for model fitting across all conditions so that an increase in the magnitude of fitting error cannot be attributed to an increased number of data points, thereby enabling meaningful comparisons of coordination variability between different conditions. To meet this requirement, the following method, based on a Monte-Carlo approach, was used. For any time window, a specific number of data frames (the same across all conditions) were randomly selected from the total number of data frames in the window. That number (called below “the size of Monte-Carlo subset”) was selected so that it was not larger than the minimal total number of data frames in the time window across all conditions. That selection was performed sixteen times (to decrease the variance of the data processing result), and each time, Model 1 was fitted to that data subset and the fitting error magnitude (the RMS value) was calculated. The average RMS value across the obtained 16 individual RMS values was used as a measure of XYC variability.

Analysis of XYC variability within the entire movement phase for an individual trial

To determine the precision of XYC approximation within the entire movement phase of an individual trial, Model 1 was applied to a data set including all data points for the given trial (Fig. 1a). The residual error magnitude was calculated for that data set as the RMS value of the residual errors and taken as a measure of intra-trial XYC variability. In fitting Model 1 to the data, the above-described Monte-Carlo method (section “[Utilization of Monte-Carlo approach for achieving consistency of coordination variability measurement](#)”) was utilized in the following steps: Step 1) based on the minimal mean movement time across all 12 conditions [i.e., 489 ms (65 frames) for the large target at short-distance condition under the maximum speed], the size of Monte-Carlo subset within each trial was determined as 65; Step 2) when fitting Model 1 to data, 65 data points were randomly selected from all data points of each trial, and the RMS value of residual errors was calculated as the fitting error magnitude; and Step 3) Step 2 was repeated 16 times, and the average RMS value across 16 RMS values was calculated and used as a measure of intra-trial variability of XYC for that trial.

Assessment of the movement phase dependence on XYC inter-trial variability

To further assess how the precision of XYC across trials within each participant changed during the course of reaching movement, the following data analysis procedure was performed (Fig. 1b). *First*, mean movement time across all trials and all participants was calculated for each condition. Subsequently, time window width T_w for model fitting was set as 20 % of that mean movement time. Specifying the time window width as specific percentage of the total movement time (rather than specific time duration) was made to have the window correspond to a specific *phase* of the movement invariant with respect to movement time duration, which varied considerably across different conditions. *Second*, Model 1 was applied to the set of data points across all trials of each participant within a time window comprising the first T_w sampling points. *Third*, the residual error magnitude was calculated within the time window as the RMS value of the residual error (i.e., square root of smallest eigenvalue divided by mean eigenvalue) and used as the measure of XYC inter-trial variability. *Fourth*, the average RMS value and its SE across all participants were calculated. *Fifth*, the second, third and fourth steps were repeated while the time window was moved forward one sampling interval at a time until the end of the window reached the end of the movement (i.e., the last T_w sampling points).

For model fitting, the above-described Monte-Carlo method (section “[Utilization of Monte-Carlo approach for achieving consistency of coordination variability measurement](#)”) was utilized according to the following procedure: Step 1) based on the minimal mean movement time across all 12 conditions [i.e., 489 ms (65 frames)], the size of Monte-Carlo subset across all trials within each participant and each condition was determined as 130 for the time window (T_w) of 20 % of the mean movement time [it was because 20 % of 65 frames yielded 13 frames per trial, which was multiplied by 10 (since there were 10 trials per condition per participant)]; Step 2) when fitting Model 1 to data, 130 data points were randomly selected from all data points of the entire time window, and the RMS value of residual errors was calculated as the fitting error magnitude; and Step 3) Step 2 was repeated 16 times, and the average RMS value across the obtained 16 individual RMS values was calculated and used as the measure of XYC variability for the entire time window.

Estimation of the extent of correlation between the end-point error components and XYC model fitting errors

To determine the extent to which the inter-trial variability of XYC reflected the inter-trial variability of the end-point position, the following analyses were performed: Step 1) the X and Y components of the end-point position error were calculated for each trial as a vector distance from the hand's final position to the center of the target for each X and Y coordinate (which are labeled here as Δx and Δy , respectively); Step 2) correlation between the model's fitting error [i.e., residual error magnitude (RMS) obtained for each data point of a data set, which is labeled here as e] and the end-point position error components (Δx and Δy) was calculated across all data points of a data set to which the model fitting was applied; and Step 3) a generalized correlation estimate (which is labeled here as r_{xy}) between the end-point error as a pair (Δx , Δy) and the model fitting error e was calculated as the square root from the R -square value corresponding to linear regression between e as a dependent variable and Δx and Δy as independent variables. The part of model fitting error not related to the end-point error was estimated as $e_{\text{adj}} = (1 - r_{xy})e$. This procedure was applied to adjust the profiles of XYC inter-trial variability obtained as described above in section “[Assessment of the movement phase dependence of XYC inter-trial variability](#)”.

Results

First, we present basic characteristics of movement kinematic and then the results of XYC analysis.

Kinematic characteristics

As expected, the participants significantly decreased movement time from the low-speed condition to the maximum-speed condition ($F(2,28) = 239.5$, $P < 0.001$, Fig. 2a, b). This change was accompanied by the increase in average movement velocity ($F(2,28) = 105.9$, $P < 0.001$, Fig. 2c, d). The movement time was significantly longer for the longer distance conditions [$F(1,14) = 163.4$, $P < 0.001$] and for the smaller target conditions [$F(1,14) = 11.7$, $P < 0.01$]. The average velocity was higher for the longer distance conditions [$F(1,14) = 56.8$, $P < 0.001$] and the larger target conditions [$F(1,14) = 54.9$, $P < 0.001$]. As can be seen in Fig. 2, distance by speed interaction was significant for the movement time [$F(2,28) = 31.8$, $P < 0.001$] and average velocity [$F(2,28) = 36.0$, $P < 0.001$]. The target size by speed interaction was also significant [$F(2,28) = 18.2$, $P < 0.001$].

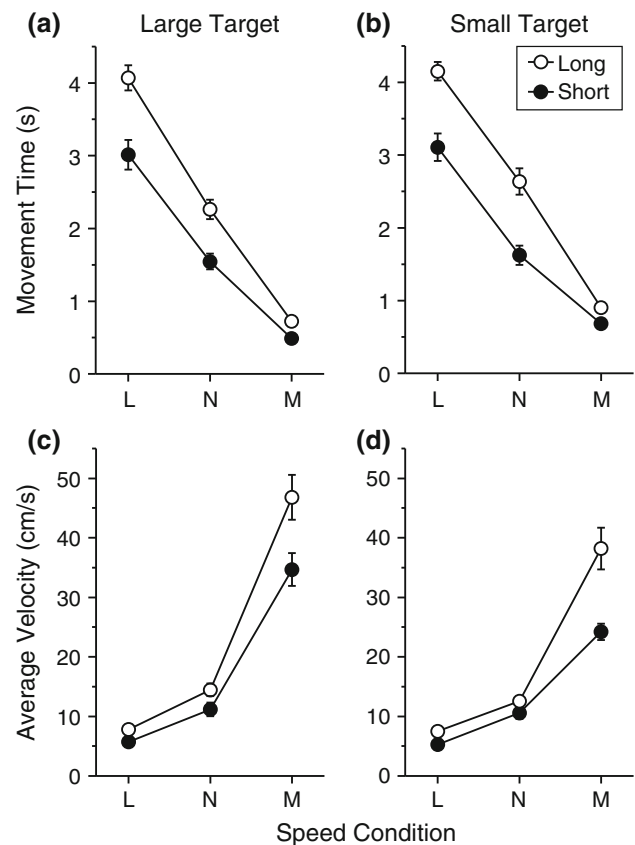


Fig. 2 Effect of speed conditions on the average movement time (a, b) and average velocity of reaching movement (c, d) across all participants. The large-target condition (a, c) and the small-target condition (b, d) are plotted separately. Filled circles refer to the short-distance condition (15 cm), and open circles refer to the long-distance condition (30 cm). L, N and M refer to low-, normal- and maximum-speed conditions, respectively. The error bars indicate the standard errors

Variability at the beginning and the end of movement

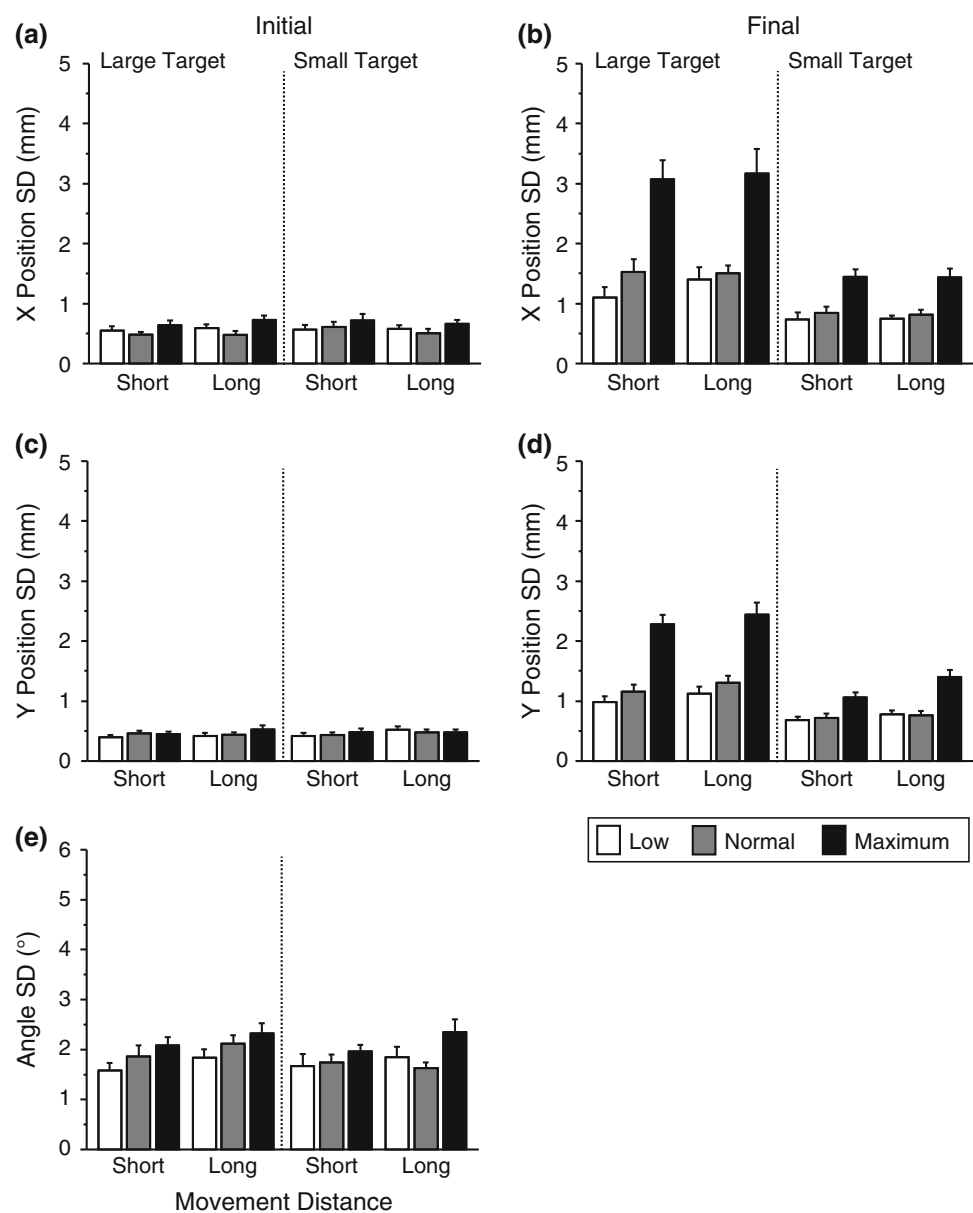
To examine how accurately the hand (i.e., the tip of the stylus) was placed on the starting position or landed on the target, the inter-trial variability of the hand's position (X and Y coordinates separately) was measured both at the initial and the final points of movement (Fig. 3a–d). In general, the initial position (a, c) was less variable than the final position (b, d) in terms of both X and Y components. The inter-trial variability of both the initial and the final hand positions significantly increased with an increase in the prescribed movement speed [initial X position: $F(2,28) = 9.2$, $P < 0.01$; final X position: $F(2,28) = 44.5$, $P < 0.001$; final Y position: $F(2,28) = 60.8$, $P < 0.001$]. A post hoc analysis showed that the inter-trial variability of

all those parameters was significantly greater under the maximum-speed condition than under either the low- or the normal-speed condition [$P < 0.05$].

The observed increase in the end-point variability under faster speed coincides with the principle of speed–accuracy trade-off. In contrast, the significant increase in initial-point variability of the X coordinate under faster speed is remarkable (Fig. 3a). This is unexpected because the hand was placed at the starting position prior to the “go”-signal, and therefore, the hand placement was not stressed by the timing demand imposed by the speed condition.

As anticipated, the large target resulted in significantly greater inter-trial variability of the final position compared to the small target for both X [$F(1,14) = 64.5$, $P < 0.001$] and Y [$F(1,14) = 121.6$, $P < 0.001$] components.

Fig. 3 Components of the variability of hand position and motion. Average inter-trial variability (across participants) of X (a, b) and Y (c, d) components is shown for the hand's initial (a, c) and final (b, d) positions. Inter-trial variability of the angle of the initial movement direction is shown in e. White, gray and black columns refer to low-, normal- and maximum-speed conditions, respectively. Short and long refer to the short- and long-reaching distance conditions, respectively. Error bars represent standard error



This increase in the end-point variability was accentuated under the faster speed conditions, leading to a significant target size by movement–speed interaction [final X position: $F(2,28) = 14.7$, $P < 0.001$, Fig. 3b; final Y position: $F(2,28) = 25.2$, $P < 0.001$, Fig. 3d]. Furthermore, a reaching distance effect was significant only for the Y component of the end-point variability [$F(1,14) = 6.9$, $P < 0.01$]. The results of the inter-trial variability of the initial direction of hand motion are shown in Fig. 3e. This parameter was significantly increased with an increase in the reaching distance [$F(1,14) = 6.9$, $P < 0.01$] and the movement speed [$F(2,28) = 5.5$, $P < 0.01$].

Factors contributing to end-point variability—correlation between the initial point and final point

To determine the extent to which the initial deviation from the starting area's center is propagated through the entire movement, the dependence of the X and Y coordinates of the movement end-point (i.e., final hand position) on the X and Y coordinates of the hand's initial position and the initial direction angle was examined by using a linear regression analysis (see details in “Methods”). The results are summarized in Table 1. The R -square value was significant for both X and Y coordinates of the final hand position when the regression analysis was performed separately for each speed condition (Table 1-I), for each target size (II) and for each reaching distance (III). The only exception was the final X position under the small-target condition (Table 1-II).

The significant correlation observed between the initial and the final hand positions indicates that the initial deviation from the starting area's center was propagated to a significant extent through the entire movement. That correlation was significantly stronger when the target was larger [the X coordinate: $P < 0.001$, Table 1-II] and when the reaching distance was shorter [both X and Y coordinates: $P < 0.01$, Table 1-III]. The more the initial deviation from the center of the starting area correlates with the end-point deviation from the center of the target area, the less correction is made during the movement. Thus, the above results indicate that the initial deviation in X direction was propagated to the hand's final position to a larger extent when the movements were either shorter or made to the larger target area. The initial deviation in Y direction was propagated to the movement's end-point to a significantly larger extent in shorter distance movements.

XYC variability within an individual trial

One of the most important characteristics of transport–aperture coordination (TAC) during reach-to-grasp movements is relatively small variability of TAC within an

Table 1 Dependence of the strength of correlation between the movement's onset and offset on prescribed speed, target size and reaching distance

	N	Final X position		Final Y position	
		R -square	Correlation coefficient	R -square	Correlation coefficient
<i>(I) Speed condition</i>					
Low	600	0.042**	0.205	0.119**	0.345
Normal	600	0.039**	0.198	0.106**	0.325
Maximum	600	0.016*	0.126	0.075**	0.273
<i>(II) Target size</i>					
Large	900	0.101**	0.318 [†]	0.075**	0.273
Small	900	0.005	0.073	0.106**	0.326
<i>(III) Reaching distance</i>					
Short	900	0.074**	0.272 [‡]	0.216**	0.465 [‡]
Long	900	0.022**	0.148	0.044**	0.21

The results have been obtained by performing linear regression analysis separately for the X and Y coordinates of the trajectory's end-point (i.e., final position), in each case using the X and Y coordinates of the initial position of the stylus and the initial movement direction angle as the independent variables

Significance of R -square value: * $P < 0.05$; ** $P < 0.001$

Significance of correlation coefficient difference between the target size-related conditions: [†] ($P < 0.001$)

Significance of correlation coefficient difference between the reaching distance-related conditions: [‡] ($P < 0.01$)

individual trial, which indicates that the precision of TAC is rather high and execution noise is quite small (Rand et al. 2010b). To determine whether XYC also has this characteristic, the XYC model was applied to data sets each of which comprised the entire movement phase for one trial (Fig. 1a, see section “Analysis of XYC variability within the entire movement phase for an individual trial”). The average magnitude of model fitting errors across all trials and all participants revealed that intra-trial variability of XYC depended on experimental conditions (Fig. 4). That variability decreased as the movement speed was increased. Accordingly, a 2 (target size: large, small) \times 2 (movement distance: short, long) \times 3 (movement speed: low, normal, maximum) \times 15 (participants) ANOVA revealed a significant movement speed effect [$F(2,1620) = 2389.0$, $P < 0.001$]. The variability was also significantly greater for the small target compared to the large target [$F(1,1620) = 53.5$, $P < 0.001$]. The intra-trial variability was significantly greater for the long-distance movement compared to the short-distance movement [$F(1,1620) = 2847.4$, $P < 0.001$].

Furthermore, as can be seen in Fig. 4, the slope of increase in the intra-trial variability from the maximum to the low-speed condition was steeper for the far-distance condition than for the near-distance condition. Accordingly,

there was a significant two-way interaction of movement speed by movement distance [$F(2,1620) = 268.0$, $P < 0.001$]. The effect of movement speed on the magnitude of the intra-trial variability of XYZ was very similar to that found for intra-trial variability of TAC during reach-to-grasp movements (Rand et al. 2010b). Moreover, it is important to note that the magnitude of XYZ intra-trial variability was very small compared to that of XYZ variability across trials (see below, section “XYZ variability across trials,” Fig. 5). This feature of XYZ variability was also typical for TAC variability.

XYZ variability across trials

The phase dependence of TAC variability across trials during reach-to-grasp movements has a specific pattern: That variability is relatively large during the initial phase, and it rapidly decreases toward the end of the movement (Rand et al. 2008). To examine whether a similar pattern of XYZ inter-trial variability dependence on the phase of the reaching movement can be also observed, Model 1 was applied to data sets related to each participant separately by using a sliding window technique with a window width of

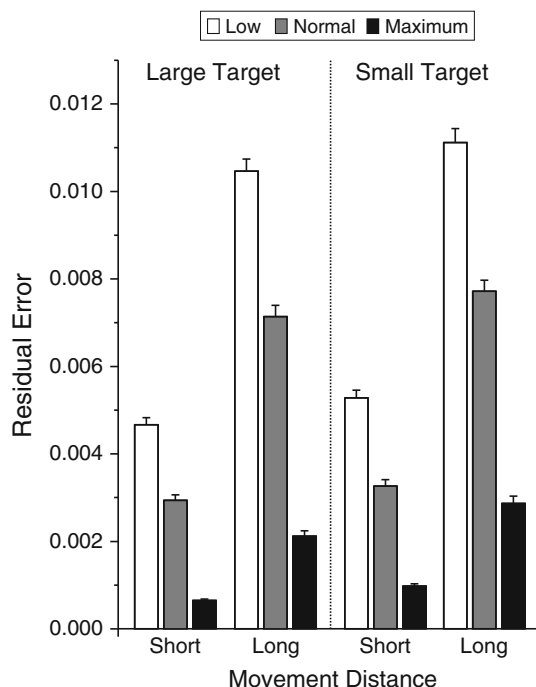


Fig. 4 Average magnitude of the residual errors of XYZ within trial approximation during the entire movement phase. The XYZ model was applied to each trial separately (i.e., to the data set comprising all data points of one trial). The average residual error magnitude across all trials and all participants is shown for each movement speed condition. White, gray and black columns refer to low-, normal- and maximum-speed conditions, respectively. Short and long refer to the short- and long-reaching distance conditions, respectively. Error bars represent standard error

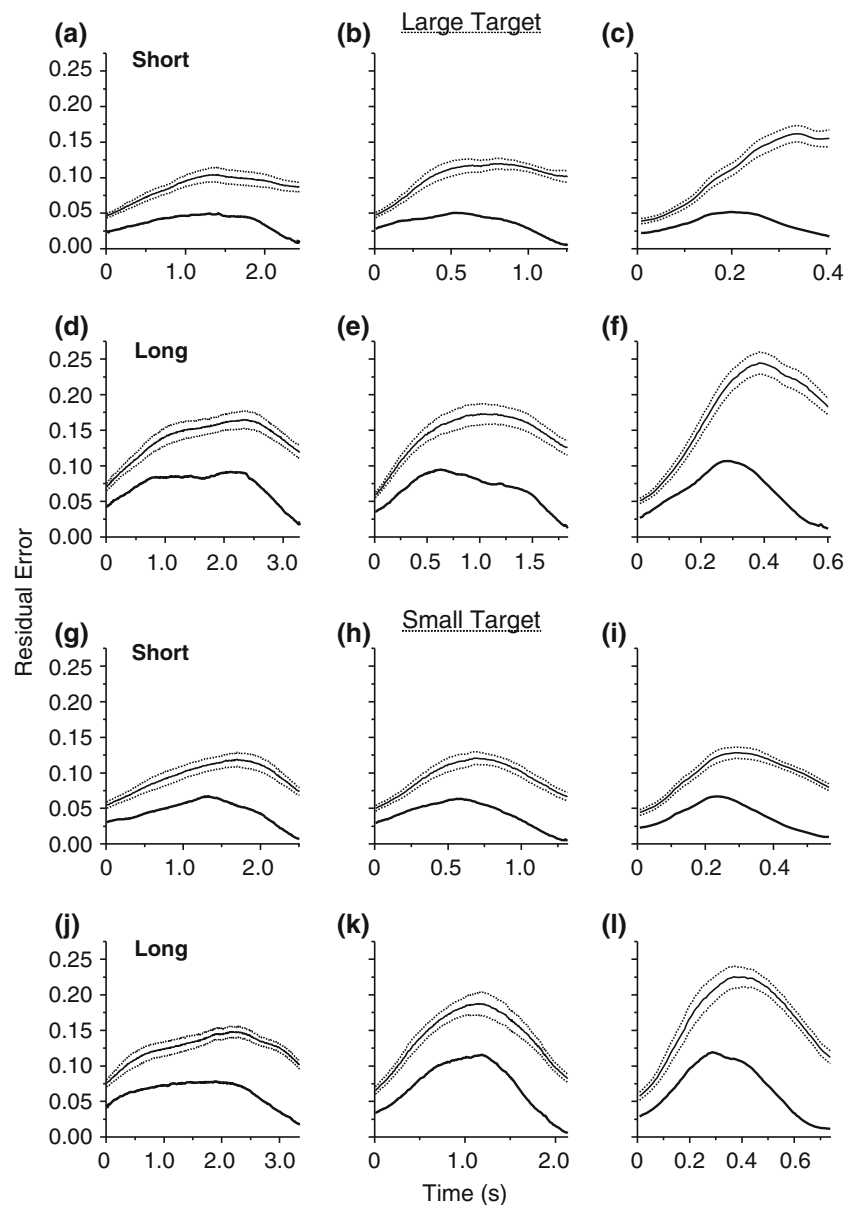
20 % of average movement time (Fig. 1b, see section “Assessment of the movement phase dependence of XYZ inter-trial variability”). An average data fitting error across participants and its SE are plotted for each of all windows throughout the movement (Fig. 5, thin lines). The thin solid lines in Fig. 5 depict the phasic changes of the variability (i.e., RMS values calculated based on the least, sixth eigenvalue) for all conditions. In general, under each condition, the XYZ inter-trial variability was the smallest at the beginning of the movement, and it gradually increased toward the middle of the movement (Fig. 5). This feature contrasted with that observed for TAC during reach-to-grasp movements, where the initial inter-trial variability was considerably larger relative to its peak (Rand et al. 2008).

The peak of the variability was greater under the faster speed conditions. The inter-trial variability of XYZ generally decreased toward the end of the movement for most conditions, indicating that optimality of the XYZ among the six movement parameters (x , y , v_x , v_y , a_x , a_y) increased as the hand approached the target. The observed decrease in the inter-trial variability was more pronounced under the small-target conditions (Fig. 5g–l) than under the large-target conditions (Fig. 5a–f). Furthermore, when short-distance movements were made to the large target, the inter-trial variability of XYZ did not decrease toward the end of the movement at all (Fig. 5a–c). These results indicate that XYZ optimality increases (and the variability of XYZ decreases) toward the end of the movement to a greater extent when higher terminal accuracy is required.

Inter-trial variability of XYZ excluding end-point variability

Assessment of the precision of information processing based on measuring the inter-trial variability of coordination hinges on an assumption that the controlled object’s state at the trajectory’s end-point (i.e., at the contact with the target object) does not vary significantly between different trials. This assumption is justified in the case of reach-to-grasp movements because relatively high precision of contact with the target object is required for successful performance of the motor task. During point-to-point reaching movements investigated in the present study, however, for successful performance, it is sufficient that the trajectory’s end-point be anywhere within the target area. In other words, the participant has no reason to reduce the end-point’s variability as long as the end-point is within the target area. Consequently, the precision of information processing can be very high during the final phase of movement control, but, due to the inter-trial variation of the end-point, the inter-trial variability of XYZ (measured as the precision of the XYZ model fitting to a

Fig. 5 Temporal modulation of XYC inter-trial variability during the entire movement phase. The results are shown for different experimental conditions related to slow (a, d, g, j), normal (b, e, h, k) and maximum (c, f, i, l) speed of reaching, as well as to short- (a–c, g–i) and long-distance (d–f, j–l) reaching amplitude. The large-target conditions (a–f) and the small-target conditions (g–l) are plotted separately. For each condition, the optimal XYC model was applied separately to different sets of data points related to each participant by using a sliding window technique with a window width of 20 % of the average movement time. The average residual error magnitude across all participants and the standard error were calculated and plotted for each position of the sliding time window. The residual error magnitude and the corresponding standard error are shown with *thin solid lines* and *dotted lines*, respectively. The *thin solid lines* refer to the XYC inter-trial, intra-subject variability that included the influence of the end-point position errors. *Thick solid lines* refer to the same variability that excluded that influence



data set comprising a number of trials) still can be significantly large.

To determine the extent to which the inter-trial variability of XYC reflected the inter-trial variability of the end-point position, correlation between the model fitting error e (obtained for each data point of a data set) and the X and Y components of the end-point position error obtained for each trial (Δx and Δy , respectively) was calculated across all data points of a data set to which model fitting was applied (see section “[Estimation of the extent of correlation between the end-point error components and XYC model fitting errors](#)” for details). To illustrate the phase dependence of that correlation, the correlation was calculated separately for each position of the sliding window that was used to fit the model of XYC (the window

width was 20 % of average movement time). The average absolute value of correlation coefficient across participants is plotted in Fig. 6 for the X and Y components separately. For all conditions, correlation between the Y component’s end-point error (Δy) and model fitting error e (dotted lines) gradually increased, usually reaching above 0.8 by the end of the movement. Thus, the inter-trial variability of XYC strongly reflected the inter-trial variability of the end-point Y position toward the end of the movement. In contrast, correlation between the X component’s end-point error (Δx) and model fitting error e (thin lines) usually fluctuated around its initial level throughout the movement.

In addition, an estimate r_{xy} of generalized correlation between the end-point error as a pair (Δx , Δy) and the XYC model fitting error e was calculated as the square root from

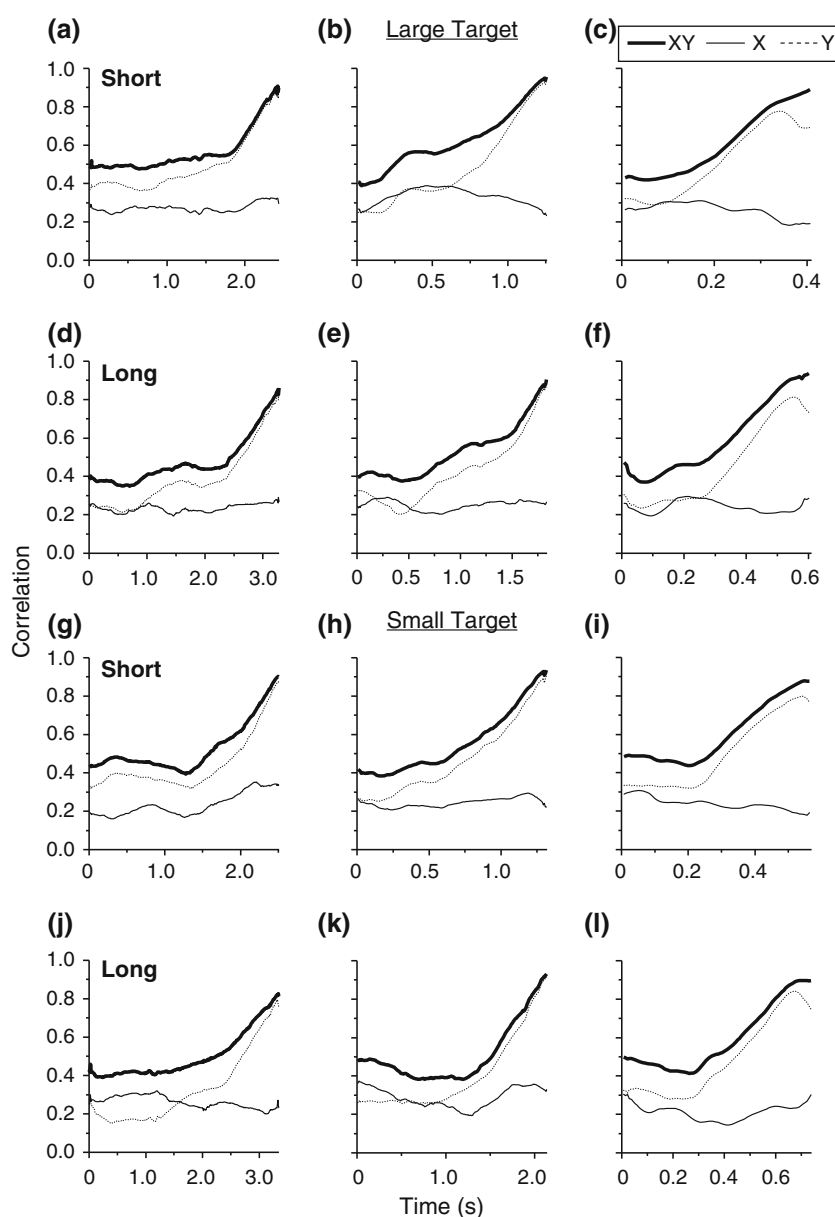
the R -square value of linear regression where Δx and Δy are independent variables and e is a dependent variable. The generalized correlation estimate gradually increased, reaching above 0.9 by the end of the movement (Fig. 6, thick lines). These results show that the inter-trial variability of XYC strongly reflects the inter-trial variability of the end-point position. The fact that the residual error of XYC model fitting correlated significantly with the end-point position indicates that the magnitude of XYC model fitting across trials reflects end-point variability rather than the precision of information processing during the final phase.

To estimate the part of the inter-trial variability of XYC that did not reflect the end-point position variability, the XYC model's adjusted fitting error was calculated as

$e_{\text{adj}} = (1 - r_{xy})e$ (Fig. 5, thick lines). Conceptually, model fitting error e_{adj} describes what the inter-trial variability of XYC would look like if the participants were hitting the center of the target area precisely for all trials. As can be seen in Fig. 5 (thick lines), the adjusted inter-trial variability of XYC decreased gradually toward the movement end for all conditions.

When the part of the inter-trial variability of XYC determined by the end-point position variability was removed, the reduction in the XYC inter-trial variability in the final phase was clear, indicating an increased precision of XYC. These profiles are very similar to those found in inter-trial variability of TAC during reach-to-grasp movements (Rand et al. 2008). Inter-trial, inter-subject variability of XYC (Fig. 5, thick lines) reveals only a very

Fig. 6 Correlation between the XYC model's fitting error and the X and Y components of the end-point position error. For each condition, a correlation coefficient of each of X (thin solid lines) and Y (dotted lines) components and a generalized correlation estimate that combined the influence of XY component errors (thick solid lines) were calculated (see details in "Methods") for different sets of data points separately. Each data set comprised all data points within a specific time window (which was equal to the 20 % of the mean movement time) across all trials performed by each participant. The time window was moved through the movement phase one data sampling point at a time. The absolute value of the average correlation coefficient across all participants for the X (thin solid line) and Y (dotted line) components and the average generalized correlation estimate (thick solid line) is plotted for each position of the sliding time window



short low-variability period at the very end of the movement. This feature was clearer under the maximum-speed conditions, especially for reaches to the small target (Fig. 5i, l), than under other conditions.

Discussion

The main goal of this study is to investigate motor coordination during point-to-point, reaching movements performed on a horizontal plane and find out whether their control strategy conforms to the general concept of two-phase control strategy evolved from the application of an optimal coordination model to reach-to-grasp movements (Rand et al. 2008, 2010b). According to the two-phase control strategy concept, the cost of information processing during motor planning and movement online control is saved during the initial phase at the expense of reduced precision of neural computations. This results in relatively large inter-trial variability of XYZ in the initial phase. In the final phase of movement control, the control precision is significantly increased to ensure sufficient precision of target acquisition at the end of the movement trajectory. This results in minimal inter-trial variability of XYZ during the final phase. Has the analysis of the experimental data obtained in the present study provided sufficient amount of evidence for the above control strategy properties?

Dependence of XYZ variability on movement phase and experimental conditions

The fact that the intra-trial variability of XYZ is very small (Fig. 4) proves that the model of XY optimal coordination fits the experimental data with high precision. It also strongly indicates that execution noise is minimal. Furthermore, if execution noise were significant, one would expect to observe larger magnitude of that noise and, therefore, greater intra-trial variability under higher movement speed. In fact, however, the extent of intra-trial variability significantly decreases with an increase in the prescribed movement speed (Fig. 4). Thus, the experimental results directly and strongly contradict the above expectations, thereby proving that execution noise was insignificant under the conditions of the described experiments.

Assessment of the variability of motor coordination across trials (inter-trial variability of XYZ) provides information about the extent of movement control optimality. In general, assuming high accuracy of target acquisition (i.e., small variability of hand trajectory's end-point), the higher is the optimality of movement control, the lower the inter-trial variability of motor coordination in

the final phase must be observed. The requirements for end-point precision in the motor task tested in the present study are determined by the size of the target area. As a result, the observed end-point variability is significant and its magnitude significantly depends on movement conditions (Fig. 3b, d). The fact that the mismatch error of the model of optimal XYZ significantly correlates across trials with the end-point position (Fig. 6) reveals that the inter-trial variability of XYZ has a large component due to the variability of the end-point position.⁵ After that component is removed, the phase dependence profile of XYZ inter-trial variability looks a lot like that in the case of reach-to-grasp movements. Namely, it showed large variability during the initial phase and rapid decrease toward the end of the movement to a level of intra-trial model fitting errors (Fig. 5, thick lines). Thus, this finding supports our hypothesis that the two-phase strategy is also utilized by the CNS for controlling planar point-to-point movements.

The current study revealed that the final phase of movement control of planar reaching, which is characterized by the very low level of the inter-trial variability of XYZ (close to the level of coordination intra-trial variability), is quite short. The strongest (i.e., most pronounced in terms of its time duration and extent to which the inter-trial variability of XYZ is decreased) final phase is observed under maximum speed (especially long-distance, small-target condition, Fig. 5c, f, i, l). In contrast, the final phase is the least pronounced under the low-speed conditions (especially short-distance, large-target condition Fig. 5a, d, g, j). Thus, the strength of the final phase varied considerably across experimental conditions.

Factors contributing to end-point variability

The dependence of the end-point variability on the prescribed movement speed shows a classical picture of speed–accuracy trade-off (Fig. 3b, d). It is remarkable, however, that not only the variability of the end-point, but also that of the initial position's *X* component significantly increased with movement speed increase (Fig. 3a) despite the fact that stylus positioning was performed before the “go”-signal, meaning that the participant had sufficient time for that positioning. It cannot be excluded that the position variability increase was due to a change in biomechanical factors, such as the way of holding the stylus or arm initial position, made in response to higher prescribed speed. At the same time, this phenomenon finds a natural explanation in the framework of the two-phase strategy

⁵ This component does not reflect any significant nonoptimality of movement control if it is determined by the variability of the end-point within the boundaries of the target area. This is so because as long as the end-point is within the target area, its deviation from the area's center does not increase the cost of a target acquisition error.

concept. Namely, the accuracy of the initial placement of stylus is lowered because the control of its initial positioning is performed under the same setting regarding speed–accuracy balance as the rest of the task performance elements. Since that balance is shifted to lower accuracy under maximum prescribed speed condition (according to the speed–accuracy trade-off principle), the initial placement is also performed with higher variability. This inference is in complete agreement with the assumption that the CNS implements a special controller that regulates the precision of neural computations required for movement control, and relaxes that precision whenever possible (see Shimansky and Rand 2012 for more details). This contention is also supported by a most recent study indicating that optimality of sensory information processing is reduced when precision requirements are reduced (Ho et al. 2012).

The requirements for end-point precision in the motor task tested in the present study are determined mostly by the size of the target area. Under the small-target condition, due to higher end-point precision requirements, the amount of movement correction is expected to be significantly greater than under the large-target condition. Consequently, the strength of correlation between the movement onset parameters and the final position of the hand must be significantly reduced under the small-target condition. This prediction is fully supported by the experimental results (Table 1-II).

The data analysis results provide information for determining the sources of the inter-trial variability of the end-point position. It has been previously suggested that execution noise is the main source of such variability (van Beers et al. 2004). Intuitively, greater execution noise is expected to be observed during more vigorous movements (i.e., performed with higher speed). Therefore, an assumption that execution noise is the main source of end-point position variability is consistent with the fact that the higher is the movement speed, the greater the variability of the *X* and *Y* coordinates of the end-point is observed (Fig. 3b, d). From a different perspective, however, if the impact of execution noise were significant, significantly less correlation between initial position and movement direction and the end-point position would be expected under faster movements. However, in a clear contradiction with this expectation, the results of the data analysis show that prescribed movement speed did not significantly affect correlation between the initial position, initial movement direction and the end-point position. This contradiction strongly indicates that execution noise was not a significant factor determining the end-point's variability. Furthermore, if execution noise were significant, it would cause significant intra-trial variability of XYZ, especially under higher movement speed, where the end-point errors are larger. The fact that the intra-trial coordination variability is the

lowest when the speed is the highest (Fig. 4) directly and very strongly contradicts that assumption. Thus, execution noise is not a significant factor contributing to the end-point variability observed in the present study.

Why then greater end-point variability is observed under higher prescribed movement speed? The significant amount of correlation observed between the initial and the final positions of the stylus (Table 1) indicates that the initial deviation from the starting area's center is propagated to a significant extent through the entire movement. For example, the fact that such correlation is significantly stronger under shorter movement amplitude (Table 1-III) confirms an intuitive expectation that less correction is performed during shorter amplitude movements. From the fact that the intra-trial variability of XYZ is lower for higher movement speed, it is evident that the higher is the prescribed movement speed, the less the initial deviation from the straight line that connects the initial hand position and the target center is corrected during the movement. Therefore, any directional deviation at the movement onset must result in greater deviation at the end-point. These interpretations are supported by a previous observation that movement deviations occurred in early phase of rapid aiming movements were propagated through the entire movement and magnified as the movement progressed (Bédard and Proteau 2004; Khan et al. 2006). Thus, there are two factors significantly contributing to the observed increase in end-point variability with an increase in the prescribed movement speed. First, the higher the movement speed is, the greater is the variability of the initial movement direction (Fig. 3e). Second, under higher movement speed, less correction of the initial directional error is made, which results in the gradual accumulation of that error through the movement.

Relationship between motor variability and XYZ variability

A decline of motor variability (i.e., the variability of the movement trajectory) during the later phase of goal-directed movements has been observed previously in terms of arm transport during the reach-to-grasp movement (Bertram et al. 2005; Haggard and Wing 1997) and arm reaching during reach-to-point movement (Khan and Franks 2003; Khan et al. 2003; Tinjust and Proteau 2009). It was shown that such reduction in the inter-trial variability of reaching trajectory was due to visual feedback-based online movement corrections (Khan and Franks 2003; Khan et al. 2003).

In the current study, the extent of the variability of XYZ was estimated as the magnitude of the error of fitting the model of optimal coordination to a given data set. The variability of XYZ (and motor coordination in general) is a

specific component of motor variability. Namely, it measures motor variability in the direction critical for movement control optimality (Shimansky and Rand 2012). In the case of reach-to-grasp movements, for example, it has been shown that, although the variability of kinematic parameters is significant in the final, aperture closure phase, the variability of *coordination* between hand transport and finger aperture is very close to zero during that phase (Rand et al. 2008). Thus, the decrease in the variability of XYZ observed toward the movement's end reflects increased optimality of movement control in the final phase, rather than a general decrease in motor variability. Note that a general increase or decrease in motor variability does not necessarily mean that the variability of motor coordination is also increased or decreased. To determine whether *coordination* variability has decreased, which would indicate an increase in the extent of movement control optimality, a special data analysis based on the model of optimal coordination is required, as performed in the current study.

The results of inter-trial variability analysis for XYZ and end-point position of the movement trajectory provide insights into understanding the CNS's movement control strategy. The increase in correlation between the fitting error of the XYZ model and the end-point position's deviation from the target area's center (Fig. 6) indicates that the amount of movement correction decreases as the target area is approached. That decrease is consistent with the central idea of the two-phase strategy concept that the CNS increases the precision of information processing at the transition from the initial phase to the final phase of movement control. Thus, the end-point deviation from the target center is not a result of some noise acting during the ongoing movement. It is already determined to a significant extent by the initial position of the stylus and the initial direction of its movement. To minimize the end-point error cost, higher precision of information processing during the final phase is used, as always. However, that cost is zero as long as the end-point is inside the target area. Hence, there is no need for the CNS to decrease the variability of the end-point within the target area. For the same reason, there is no need to decrease the related part of the inter-trial variability of XYZ. When that part is removed from the variability of XYZ during the final phase, XYZ variability during that phase is minimal, just as expected according to the two-phase strategy concept.

Theoretical implications

Optimality approach

An optimality approach has been traditionally applied to the movement trajectory (e.g., Viviani and Flash 1995).

This application is based on an implicit assumption that, since a given motor task is well optimized through extensive training, the movement trajectory is also optimized to the same extent. The current model of optimal XYZ is formulated in terms of movement kinematic variables expressed based on *X* and *Y* spatial coordinates, assuming that movement control is optimal. Apart from that assumption, analyzing how exactly movements are planned is beyond the scope of this study. For example, there are many existing theories of how reaching movements are planned, such as vector-coding (e.g., Vindras and Viviani 1998), minimization process (Yang and Feldman 2010) and force control (Kawato 1999, Wolpert and Ghahramani 2000). We believe that our model in general is compatible with any existing control concept as long as it assumes optimization of movement control according to a certain criterion.

Movement control optimization and variability

If the movement trajectory is ideally well optimized, there is no room for its variability. Consequently, in the literature on arm movement control, motor variability is usually regarded as an inherent noise that is a negative factor, and the control system has to decrease it for improving the performance of motor tasks (Faisal et al. 2008; Harris and Wolpert 1998; Khan et al. 2006; Newell and Corcos 1993; Todorov and Jordan 2002). An optimal feedback control concept has been proposed, according to which the optimality criterion should include the cost of errors in task performance caused by motor variability (Todorov and Jordan 2002). To minimize that cost, the CNS decreases motor variability in the directions critical for the quality of task performance. The optimal feedback theory, however, does not explain how the CNS manages to suppress the inherent noise, although some of the CNS's mechanisms possibly employed for noise reduction have been suggested recently (Bays and Wolpert 2007). By utilizing a quantitative model of optimal XYZ for experimental data analysis, it has been demonstrated in this study that execution noise is insignificant (section "[XYZ variability within an individual trial](#)") and, therefore, cannot be responsible for the observed inter-trial variability of reaching movements. The two-phase strategy concept provides the following alternative explanation for that variability. First, the state of the controlled object (primarily the reaching extremity) at the movement onset significantly varies from trial to trial. Second, since the CNS lowers the demand for information processing precision during the initial phase of movement control, a significant error in the movement control system's estimate of the controlled object's state is likely. That error is the main reason for the motor variability. A detailed

theoretical analysis and discussion of this mechanism can be found in (Shimansky and Rand 2012).

Two-component control of aiming movement versus two-phase control strategy

In the history of movement control research, the existence of two distinct movement components one of which is “ballistic” and the other is “corrective” was noticed in aiming movements a long time ago (Woodworth 1899). The two-component movement control model has been attracting a lot of interest ever since (Elliott et al. 2001; Khan et al. 2006). There is a striking similarity between the idea of two-phase strategy of coordination among movement parameters and the concept of two components of reaching movements. However, these two concepts were developed independently from different theoretical viewpoints, and a different methodology was employed for identifying the two components (Fradet et al. 2008; Khan et al. 1998; Meyer et al. 1988; Tinjust and Proteau 2009). Thus, it is important to determine how well the ballistic and the corrective components described in two-component concept match the initial and the final phase from our concept of the two-phase control strategy, respectively. Our planned companion paper (Part II) will address this issue.

Conclusions

Overall, the features of the movement control strategy revealed by the data analysis in this study are very similar to those found in our earlier studies on reach-to-grasp movements. In addition, it has been found that separation between the initial and the final phases of the reaching movement is best defined under conditions where both high movement speed and high end-point precision are required. Conversely, under relaxed requirements for movement speed and end-point precision, the final phase may not be completely present. These findings are in a perfect agreement with a hypothesis (which is central to the two-phase control strategy concept) that the CNS actively regulates the demand for the precision of information processing to optimize the cost of motor task performance.

The current study took the first distinct step toward the generalization of the two-phase control strategy concept from reach-to-grasp movements to planar point-to-point reaching movements. The current study is focused on movements performed in the same direction in each trial. Further generalization to wider ranges of experimental conditions is an important direction for future studies.

Appendix

Derivation of experimentally verifiable equations describing optimal coordination

The total cost of task performance Q can be presented as a sum of the following components.

$$Q = Q_M + Q_T + Q_E, \quad (3)$$

where Q_M is the cost of movement execution (mostly the cost of active force generation by muscles), Q_T is the cost of movement time duration, and Q_E is the cost of errors in making a contact with the target object. More precisely,

$$Q_M = \int_0^T (q_M[S(t), U(t)]) dt, \quad (4)$$

$$Q_T = \int_0^T (q_T[S(t)]) dt. \quad (5)$$

and Q_E is a function of the controlled object’s state $S(T)$ at the movement’s end-point. Here, q_M is the rate of spending metabolic energy on muscle contraction for generating limb moving forces. It depends on the state $S(t)$ of the limb as a controlled object and the vector of control actions $U(t)$. The cost of time duration Q_T is determined by the behavioral context in which the motor task is performed. It can vary from being very high (e.g., in dangerous situations requiring fast motor actions) to being negligible compared to other cost components. In general, the rate q_T of time duration cost significantly depends on the controlled object’s state. In relatively simple cases, it can be considered constant throughout the movement, so that $Q_T = q_T \cdot T$. The movement duration T in most cases should be considered an unprescribed and thus requiring optimization parameter (for a more detailed discussion see Shimansky 2000; Shimansky et al. 2004). The cost of end-point errors Q_E is fully determined by the motor task and the strategy of its performance. In real situations, it can be extremely high (e.g., during rock climbing).

Thus, the optimal control problem has a standard setup (e.g., Davis 2002) with the optimality criterion

$$Q(U) = \int_0^T (q_M[S(t), U(t)] + q_t[S(t)]) dt + Q_E[S(T)] \quad (6)$$

and control object’s dynamics

$$\frac{dS}{dt}(t) = F[S(t), U(t)], \quad (7)$$

which means that its solution can be described as the following equation system

$$U = H(S, S_T, T), \quad (8)$$

where U is an m -dimensional vector of control actions (each of which corresponds to a specific controlled freedom degree), S is an n -dimensional ($m \leq n$) vector fully describing the state of the controlled object at a specific point in time, S_T is an n -dimensional destination state vector, and T is time duration of movement between S and S_T . Note that the equation system 8 holds for each time point of the movement. It is assumed here that movement time duration is not prescribed, and therefore, T is a result of movement control optimization. Therefore, T is essentially the (optimal) amount of time remained to movement finish. Very importantly, since all m control processes are assumed to finish concurrently, T is *the same* for each process (i.e., for each one of the m equations).

By solving the above equation system with respect to T and excluding T from it, one obtains a reduced system of $(m - 1)$ equations,

$$G(S, S_T, U) = 0, \quad (9)$$

where G is an $(m - 1)$ -dimensional vector function.

From a geometrical perspective, these $(m - 1)$ equations describe an $(n + m - 1)$ -dimensional hypersurface in the $(n + m)$ -dimensional space, which is a composition of the controlled object's state space and the space of control actions. This combined space is a state space of the entire movement control system in which the experimenter observes it.

If S_T is the same in every trial (i.e., is a vector of constant parameters) performed under a specific condition, the above equation system (Eq. 9) can be simplified:

$$G(S, U) = 0. \quad (10)$$

The equation system 10 constitutes a model of optimal coordination. From the perspective of data analysis, the left-hand parts of these equations are functions with unknown parameters that are to be found by best fitting the model to the experimental data. Note that an alternative approach to model fitting consists in the following procedure. First, the unknown coefficients in the functions included in Eqs. 6 and 7 have to be identified. Second, the optimal control problem should be solved. Third, an optimal coordination model should be obtained as described above, resulting in an equation system 10 with coefficients calculated using those identified for Eqs. 6 and 7. This alternative route of model development is arguably much more computationally complicated. Conversely, the "short-cut" approach, namely best fitting a model in the form of equation system 10, which produces the same result, is much easier computationally. Its other important advantage is that no assumptions regarding the exact formula for the optimality criterion (a highly debatable matter) are required.

According to the general derivation procedure presented above, to derive a mathematical model of XY coordination, control actions for regulating hand motion components corresponding to X and Y coordinates can be presented as related hand transport acceleration components. Optimal coordination between two control processes is described by a system of a single equation. In the case of XY coordination, such a system describing optimal XYC can be obtained from Eq. 10 by defining the state vector as $S = [x, y, v_x, v_y]$ and the vector of control actions as $U = [a_x, a_y]$:

$$f(x, y, v_x, v_y, a_x, a_y) = 0, \quad (11)$$

where a_x , and a_y are acceleration components, and v_x , and v_y are velocity components.

Estimation of fitting errors for the XY optimal coordination model

The simplest implementation of the model of optimal XYC is linear:

$$k_x x + k_y y + k_{v_x} v_x + k_{v_y} v_y + k_{a_x} a_x + k_{a_y} a_y + k_0 = 0, \quad (12)$$

where k_x , k_y , k_{v_x} , k_{v_y} , k_{a_x} , k_{a_y} and k_0 are constant coefficients that are not simultaneously equal to zero. Note that an equation $k_x x + k_y y + 1 = 0$ describing a straight line is a particular case of Eq. 12, which means that, if the movement trajectory is a straight line segment, it satisfies the conditions for optimal XYC. Since the Eq. 12 is appreciably more general, it can be satisfied even if the movement trajectory is not straight.

The last coefficient k_0 in Eq. 12 can be excluded by scaling the movement parameters so that their respective mean values (across the data set) are all zero. Then, the model becomes a bit simpler:

$$k_x x + k_y y + k_{v_x} v_x + k_{v_y} v_y + k_{a_x} a_x + k_{a_y} a_y = 0. \quad (13)$$

This general equation actually stands for an equation system where each individual equation includes movement parameters corresponding to a specific point in time from a specific trial performed by a specific participant. All such points comprise a data set to which the model is fitted. In each case of model fitting described in this study, the number of equations in the above equation system is several times greater than the number of (unknown) coefficients, meaning that the equation system is considerably overdetermined. In general, in such cases, there is no set of coefficients that can make all the equations satisfied exactly. Therefore, the parameter identification problem is usually solved according to the principle of maximum likelihood, which, assuming quasi-normality of the probability distribution for the movement parameters across the data set, leads to a requirement that

the sum of mismatch error squares across the equations be minimal (least squares criterion):

$$\sum_{i=1}^N (k_x x + k_y y + k_{v_x} v_x + k_{v_y} v_y + k_{a_x} a_x + k_{a_y} a_y + k_0)^2 \rightarrow \min \quad (14)$$

The linear equation describing the model of optimal XYC has a trivial solution where all coefficients are equal to zero. That solution is unwanted because it does not impose any constraints on the relationship between the movement parameters. To exclude that solution, it is necessary to require that not all those coefficients be equal to zero at the same time. That requirement is usually expressed as an additional equation

$$k_x^2 + k_y^2 + k_{v_x}^2 + k_{v_y}^2 + k_{a_x}^2 + k_{a_y}^2 = 1. \quad (15)$$

The mathematical problem described by the equation system 14 and 15 is well known from the theory of principal component analysis (e.g., Jolliffe 2002). There are exactly $N = 6$ minima of the objective function (defined by the expression Eq. 14), which are given by the eigenvalues of the covariance matrix of the movement parameters. The corresponding solutions with respect to the model's coefficients are the eigenvectors of that matrix. Thus, the eigenvector corresponding to the least eigenvalue (i.e., to the global minimum of the objective function) is the result of model best fitting. The resulting values of the model's coefficients can be used to obtain the model's fitting error for any specific vector of the six movement parameters (x, y, v_x, v_y, a_x, a_y), that is, for any specific data set element.

Based on the above considerations, the fitting error for the linear implementation of the XYC model was calculated according to the following procedure.

1. The covariance matrix for the six movement parameters was calculated for the data subset to which the model was to be fit.
2. The eigenvalues of that matrix were determined (by using a standard procedure). Note that the sum of the eigenvalues is equal to the sum of the diagonal elements of the covariance matrix, that is, to the sum of the movement parameter variances.
3. The fitting error magnitude was calculated as a square root of the smallest eigenvalue divided by the mean eigenvalue (across all the eigenvalues). This division was performed to make the fitting error estimate independent of the extent of movement parameter variance (i.e., the extent of their variability). That independence is important for comparing the fitting error magnitude (used as an estimate of XYC variability) between different movement phases,

different conditions, etc. By taking the square root, the fitting error estimate was made compatible with the usual root mean square (RMS) measure of mismatch error magnitude.

Note that the obtained estimate of fitting error magnitude is dimensionless. Its upper bound is equal to 1, which corresponds to the absence of any correlation among the movement parameters.

Acknowledgments We thank Dr. Herbert Heuer for his helpful comments on an earlier version of the manuscript. We also thank Eva Hanisch, Maia Iobidze, Jennifer Stube and Sarah Jacob for their help in data collection.

References

- Bays PM, Wolpert DM (2007) Computational principles of sensorimotor control that minimize uncertainty and variability. *J Physiol* 578:387–396
- Bédard P, Proteau L (2004) On-line vs. off-line utilization of peripheral visual afferent information to ensure spatial accuracy of goal-directed movements. *Exp Brain Res* 158:75–85
- Bernier PM, Chua R, Franks IM (2005) Is proprioception calibrated during visually guided movements? *Exp Brain Res* 167:292–296
- Bertram CP, Lemay M, Stelmach GE (2005) The effect of Parkinson's disease on the control of multi-segmental coordination. *Brain Cogn* 57:16–20
- Darling WG, Stephenson M (1993) Directional effects on variability of upper limb movements. In: Newell KM, Corcos DM (eds) *Variability and motor control*. Human Kinetics, Champaign, pp 65–88
- Davis JH (2002) *Foundations of deterministic and stochastic control*. Birkhäuser, Boston
- Elliott D, Helsen WF, Chua R (2001) A century later: Woodworth's (1899) two-component model of goal-directed aiming. *Psychol Bull* 127:342–357
- Faisal AA, Selen LP, Wolpert DM (2008) Noise in the nervous system. *Nat Rev Neurosci* 9:292–303
- Fradet L, Lee G, Dounskaia N (2008) Origins of submovements during pointing movements. *Acta Psychol (Amst)* 129:91–100
- Haggard P, Wing AM (1997) On the hand transport component of prehensile movements. *J Mot Behav* 29:282–287
- Harris CM, Wolpert DM (1998) Signal-dependent noise determines motor planning. *Nature* 394:780–784
- Heuer H, Hegele M (2008) Adaptation to visuomotor rotations in younger and older adults. *Psychol Aging* 23:190–202
- Hinder MR, Riek S, Tresilian JR, de Rugy A, Carson RG (2010) Real-time error detection but not error correction drives automatic visuomotor adaptation. *Exp Brain Res* 201:191–207
- Ho T, Brown S, van Maanen L, Forstmann BU, Wagenmakers EJ, Serences JT (2012) The optimality of sensory processing during the speed-accuracy tradeoff. *J Neurosci* 32:7992–8003
- Hoff B, Arbib MA (1993) Models of trajectory formation and temporal interaction of reach and grasp. *J Mot Behav* 25:175–192
- Jolliffe IT (2002) *Principal component analysis*. Series: Springer series in statistics. Springer, New York
- Kawato M (1999) Internal models for motor control and trajectory planning. *Curr Opin Neurobiol* 9:718–727
- Khan MA, Franks IM (2003) Online versus offline processing of visual feedback in the production of component submovements. *J Mot Behav* 35:285–295

- Khan MA, Franks IM, Goodman D (1998) The effect of practice on the control of rapid aiming movements: evidence for an interdependency between programming and feedback processing. *Q J Exp Psychol A* 51:425–443
- Khan MA, Lawrence G, Fourkas A, Franks IM, Elliott D, Pembroke S (2003) Online versus offline processing of visual feedback in the control of movement amplitude. *Acta Psychol (Amst)* 113:83–97
- Khan MA, Franks IM, Elliott D, Lawrence GP, Chua R, Bernier PM, Hansen S, Weeks DJ (2006) Inferring online and offline processing of visual feedback in target-directed movements from kinematic data. *Neurosci Biobehav Rev* 30:1106–1121
- Meyer DE, Abrams RA, Kornblum S, Wright CE, Smith JEK (1988) Optimality in human motor performance: ideal control of rapid aimed movements. *Psychol Rev* 95:340–370
- Naslin P (1969) *Essentials of optimal control*. Boston Technical Publishers, Cambridge
- Newell KM, Corcos DM (1993) Issues in variability and motor control. In: Newell KM, Corcos DM (eds) *Variability and motor control*. Human Kinetics, Champaign, pp 1–12
- Papoulis A (1990) *Probability and statistics*. Prentice-Hall, Englewood Cliffs
- Rand MK, Smiley-Oyen AL, Shimansky YP, Bloedel JR, Stelmach GE (2006) Control of aperture closure during reach-to-grasp movements in Parkinson's disease. *Exp Brain Res* 168:131–142
- Rand MK, Shimansky YP, Hossain ABM, Stelmach GE (2008) Quantitative model of transport-aperture coordination during reach-to-grasp movements. *Exp Brain Res* 188:263–274
- Rand MK, Lemay M, Squire LM, Shimansky YP, Stelmach GE (2010a) Control of aperture closure initiation during reach-to-grasp movements under manipulations of visual feedback and trunk involvement in Parkinson's disease. *Exp Brain Res* 201:509–525
- Rand MK, Shimansky YP, Hossain ABMI, Stelmach GE (2010b) Phase dependence of transport-aperture coordination variability reveals control strategy of reach-to-grasp movements. *Exp Brain Res* 207:49–63
- Rand MK, Van Gemmert AWA, Hossain ABMI, Shimansky YP, Stelmach GE (2012) Control of aperture closure initiation during trunk-assisted reach-to-grasp movements. *Exp Brain Res* 219:293–304
- Shimansky YP (2000) Spinal motor control system incorporates an internal model of limb dynamics. *Biol Cybern* 83:379–389
- Shimansky YS, Rand MK (2012) Two-phase strategy of controlling motor coordination determined by task performance optimality. *Biol Cybern* (in press)
- Shimansky YP, Kang T, He J (2004) A novel model of motor learning capable of developing an optimal movement control law online from scratch. *Biol Cybern* 90:133–145
- Teasdale N, Bard C, Fleury M, Young D, Proteau L (1993) Determining movement onsets from temporal series. *J Mot Behav* 25:97–106
- Tinjust D, Proteau L (2009) Modulation of the primary impulse of spatially-constrained video-aiming movements. *Hum Mov Sci* 28:155–168
- Todorov E, Jordan MI (2002) Signal-dependent noise determines motor planning. *Nat Neurosci* 5:1226–1235
- Valero-Cuevas FJ, Venkadesan M, Todorov E (2009) Structured variability of muscle activations supports the minimal intervention principle of motor control. *J Neurophysiol* 102:59–68
- van Beers RJ, Haggard P, Wolpert DM (2004) The role of execution noise in movement variability. *J Neurophysiol* 91:1050–1063
- Vindras P, Viviani P (1998) Frames of reference and control parameters in visuomanual pointing. *J Exp Psychol Hum Percept Perform* 24:569–591
- Viviani P, Flash T (1995) Minimum-jerk, two-thirds power law, and isochrony: converging approaches to movement planning. *J Exp Psychol Hum Percept Perform* 21:32–53
- Wang J, Sainburg RL (2005) Adaptation to visuomotor rotations remaps movement vectors, not final positions. *J Neurosci* 25:4024–4030
- Wolpert DM, Ghahramani Z (2000) Computational principles of movement neuroscience. *Nat Neurosci* 3:1212–1217
- Woodworth RS (1899) The accuracy of voluntary movement. *Psychol Rev* 3(Suppl 2):1–114
- Yang F, Feldman AG (2010) Reach-to-grasp movement as a minimization process. *Exp Brain Res* 201:75–92